



Minerva Access is the Institutional Repository of The University of Melbourne

Author/s:

Tay, JH;Porter, AF;Wirth, W;Duchene, S

Title:

The Emergence of SARS-CoV-2 Variants of Concern Is Driven by Acceleration of the Substitution Rate

Date:

2022-02-01

Citation:

Tay, J. H., Porter, A. F., Wirth, W. & Duchene, S. (2022). The Emergence of SARS-CoV-2 Variants of Concern Is Driven by Acceleration of the Substitution Rate. *Molecular Biology and Evolution*, 39 (2), <https://doi.org/10.1093/molbev/msac013>.


Persistent Link:

<https://hdl.handle.net/11343/302116>

License:

CC BY

The Emergence of SARS-CoV-2 Variants of Concern Is Driven by Acceleration of the Substitution Rate

John H. Tay, Ashleigh F. Porter, Wytamma Wirth, and Sebastian Duchene *

Peter Doherty Institute for Infection and Immunity, University of Melbourne, Melbourne, VIC, Australia

*Corresponding author: E-mail: sduchene@unimelb.edu.au.

Associate editor: Thomas Leitner

Abstract

The ongoing SARS-CoV-2 pandemic has seen an unprecedented amount of rapidly generated genome data. These data have revealed the emergence of lineages with mutations associated to transmissibility and antigenicity, known as variants of concern (VOCs). A striking aspect of VOCs is that many of them involve an unusually large number of defining mutations. Current phylogenetic estimates of the substitution rate of SARS-CoV-2 suggest that its genome accrues around two mutations per month. However, VOCs can have 15 or more defining mutations and it is hypothesized that they emerged over the course of a few months, implying that they must have evolved faster for a period of time. We analyzed genome sequence data from the GISAID database to assess whether the emergence of VOCs can be attributed to changes in the substitution rate of the virus and whether this pattern can be detected at a phylogenetic level using genome data. We fit a range of molecular clock models and assessed their statistical performance. Our analyses indicate that the emergence of VOCs is driven by an episodic increase in the substitution rate of around 4-fold the background phylogenetic rate estimate that may have lasted several weeks or months. These results underscore the importance of monitoring the molecular evolution of the virus as a means of understanding the circumstances under which VOCs may emerge.

Key words: SARS-CoV-2 molecular evolution, variants of concern, molecular clock, Bayesian model selection.

Introduction

The Molecular Clock of SARS-CoV-2

Genome sequence data of viruses have been extensively used to track the evolution and spread of these pathogens. The ongoing SARS-CoV-2 pandemic has seen an unprecedented number of genomes generated that have been used to gain rapid insight to understand epidemiological spread (Dellicour *et al.* 2021), identify the time of origin (Pekar *et al.* 2021), and track mutations of functional importance. Most concerning mutations occur in the spike protein and may increase transmissibility (Kraemer *et al.* 2021), or disease severity (Harvey *et al.* 2021), although vaccines are likely still effective against them (Dearlove *et al.* 2020). Such lineages are known as variants of concern (VOCs) and they are characterized at a genomic level by a number of fixed mutations in the S1 subunit of the spike protein, the most common of which are mutations N501Y and D614G (Eurosurveillance Editorial Team 2021), with the latter presenting evidence of increased transmissibility and favored by selection (Martin *et al.* 2021; Volz *et al.* 2021). For a lineage to be formally denominated as a VOC, there must be evidence of an impact in transmissibility, virulence, and/or immunity (Mascola *et al.* 2021).

SARS-CoV-2 lineages are classified using a dynamic nomenclature system, known as PANGO (Rambaut *et al.* 2020). Recently the World Health Organization assigned

VOCs letters of the Greek alphabet (Konings *et al.* 2021). In October 2021, the United States CDC recognizes four VOCs: Alpha (PANGO lineage B.1.1.7) first identified in the United Kingdom, Beta (PANGO lineage B.1.351) first identified in South Africa, Gamma (PANGO lineage P.1) first identified in Brazil, and Delta (PANGO lineage B.1.617.2) first identified in India (CDC 2021). As of December 2021, a new VOC has been detected and has rapidly spread globally (Viana *et al.* 2022), Omicron (PANGO lineages BA.1 and BA.2), not included in this study.

The mechanisms under which VOCs have emerged is not entirely clear, but their defining mutations are well characterized and their fixation has been attributed to the action of natural selection (Martin *et al.* 2021). Variant Alpha has 14 protein-altering mutations and three deletions, with eight of these being in the spike protein. One of the deletions Δ H69/ Δ V70 enhances infectivity in vitro and has been detected in immunocompromised patients where immune escape occurred (Kemp *et al.* 2021; Plante *et al.* 2021). Variant Beta has nine protein-altering mutations with five altering the receptor binding domain. (Tegally *et al.* 2021). Variant Gamma has 17 mutations, with 10 found in the spike protein and including N501Y and E484K (Faria *et al.* 2021). Alpha, Beta, and Gamma share several important mutations, including N501Y and E404K, which likely enhance affinity to human the ACE2 receptor (Nelson *et al.* 2021). Variant Delta is

characterized by seven mutations in the spike protein, several of which have been associated with altered immune response and increased viral replication, viral load, and likely leading to increased viral fitness (CDC 2021).

The sheer number of mutations observed in these four VOCs is much higher than what would be expected under phylogenetic estimates of the nucleotide evolutionary rate of SARS-CoV-2, which range from around 7×10^{-4} to 1.1×10^{-3} subs/site/year (Duchene et al. 2020; Ghafari et al. 2022), meaning that only about two mutations along the genome would accumulate per month along a lineage. In these circumstances, the 14 mutations in Alpha would require a period of at least 6 months, a time that is inconsistent with its first detection in September 2020, because it would have had to evolve from around March 2020 with most defining mutations undetected for many months.

We investigated whether the emergence of VOCs is associated with an increase in the evolutionary rate that can be detected using phylogenetic analyses of genome data and in the absence of dense intrahost or transmission chain sampling. The term “evolutionary rate” refers to the amount of molecular change that can be measured using a phylogenetic method and is thus the result of the instantaneous mutation rate and the substitution rate (i.e. the rate at which such mutations become fixed) (Ho et al. 2011). The latter is largely determined by the action of natural selection, which is a probable cause for the large number of mutations in VOCs (Martin et al. 2021). Thus, here we use the term “substitution rate”, which reflects our estimates more closely. We analyzed publicly available nucleotide sequence data from GISAID (Elbe and Buckland-Merrett 2017; Shu and McCauley 2017) under a range of molecular clock models that describe the substitution rate along branches in phylogenetic trees, shown in the Supplementary Material online. We consider each model as a hypothesis for which we can assess statistical support using Bayesian model selection techniques. Critically, our analyses do not intend to detect signatures of natural selection, nor to identify genomic regions with higher mutation rates, which have been described elsewhere (Abdool Karim and de Oliveira 2021; Harvey et al. 2021; Martin et al. 2021). Instead, our framework serves to characterize the main patterns of substitution rate variation in the genome of the virus that underpin the emergence of VOCs.

The simplest molecular clock model is known as the strict molecular clock (SC; Zuckerkandl and Pauling 1962, 1965) that posits a single substitution rate for all branches in a phylogenetic tree, and thus serves as a “null” model. A more complex model is the uncorrelated relaxed clock that assumes that branch rates are independent and identically distributed draws from a statistical distribution (Drummond et al. 2006), for which we considered either a lognormal or a Γ distribution (UCLN and UCG, respectively). We also considered a range of fixed local clock (FLC) models (Yoder and Yang 2000). These models require an a priori definition of a set of “background” branches and a set of branches with different rates, known as “foreground.” For example, foreground branches can be defined based on some biological expectation (e.g., Worobey et al. 2014) and represent a formal

evolutionary hypothesis. The substitution rate is constant for a given group of branches, although there exist approaches where branches can be assigned a set of relaxed molecular clocks (Fourment and Darling 2018). These models differ in their number of parameters and biological assumptions (supplementary table S1, Supplementary Material online; reviewed in Bromham et al. [2018] and Ho and Duchène [2014]).

We specified six configurations of the FLC model, where the substitution rate could vary within VOC clades (FLC clades model in supplementary fig. S1, Supplementary Material online) or along the stem (FLC stems + clades), only at stem branches (FLC stems), or where these rates could be shared among all VOCs (FLC shared stems, FLC shared clades, and FLC shared clades + stems in supplementary fig. S1, Supplementary Material online).

Models in which the rate only changes along the stem branches of VOCs represent a situation where the substitution rate may increase for a short period of time before returning to the background rate. In contrast, models where the clade also undergoes a rate change would imply that VOCs have a rate that is statistically different from the background.

An alternative approach to the FLC is the random local clock (RLC; Drummond and Suchard 2010). The substitution rate can change at particular nodes in the tree and the location of such changes and actual rates are inferred. The RLC is a general form of all local clock models, where the simplest form is the SC, as a case of no rate changes (Ho and Duchène 2014; Bromham et al. 2018).

Bayesian Hypothesis Testing

We conducted Bayesian model testing by calculating the log marginal likelihood, a measure of statistical fit, and ranking the models accordingly. The difference in log marginal likelihoods between two models is known as the log Bayes factor (BF; Sinsheimer et al. 1996) and measures the relative support for two models given the data. In general, a log BF of at least 1.1 is considered as “substantial evidence” in favor of a model, with 2.3 being “strong” and 4.6 “decisive” (Kass and Raftery 1995). We considered two marginal likelihood estimators, path sampling and stepping-stone sampling (Gelman and Meng 1998; Lartillot and Philippe 2006; Xie et al. 2011).

Results

Model Selection

The FLC-shared stems model had the highest statistical fit, with a log BF of at least 1.92 compared with the next best-fitting model (2.30 with path sampling and 1.92 with stepping-stone sampling; table 1). The next model with highest mean log marginal likelihood was the UCG, followed by the FLC stems and UCLN. Note, however, that there is some overlap in replicate log marginal likelihoods for these four models (fig. 1). The top two FLC models assume that the stem branches of VOC have a rate that differs from the background and they only differ in that the FLC stems model allows each VOC stem branch to have its own rate.

Table 1. Model Selection Results for Complete SARS-CoV-2 Genomes.

Model	ps logML	ss logML	ps Rank	ss Rank	ps BF	ss BF
FLC shared stems	−55430.85	−55431.49	1	1	0	0
UCG	−55433.15	−55433.41	2	2	−2.30	−1.92
FLC stems	−55434.05	−55434.51	3	3	−3.2	−3.02
UCLN	−55435.83	−55435.81	4	4	−4.98	−4.32
SC	−55444.05	−55444.59	5	5	−13.20	−13.10
FLC shared clades + stems	−55444.77	−55445.31	6	6	−13.92	−13.82
FLC shared clades	−55449.82	−55450.29	7	7	−18.97	−18.80
FLC clades + stems	−55453.62	−55454.09	8	8	−22.77	−22.60
FLC clades	−55458.51	−55459.06	9	9	−27.66	−27.57

NOTE.—Mean estimates of log marginal likelihoods using path sampling and stepping-stone (ps logML and ss logML, respectively), over ten replicates. Log BFs are shown for the best-fitting model, relative to all others (increasingly negative numbers mean lower statistical fit), and thus they are 0.0 for the top model.

The uncorrelated relaxed clocks had very similar performance, although both had at least “substantial evidence” against them with respect to the FLC-shared stems model (i.e. $\log \text{BF} > -1.1$). The log BFs for the remaining models were at least -13 , implying “decisive” evidence against them, relative to the FLC-shared stems.

Interestingly, FLC models where VOC clades were defined as foreground had decisively lower statistical performance than those where only stem branches were labeled as foreground (table 1, fig. 1). In fact, even the SC model, which is generally considered unrealistic for empirical data, had a log BF of at least 4 with respect to FLC shared clades and the FLC clades + stems (table 1).

Rates of Evolution of Variants of Concern

The FLC shared stems model had a mean background substitution rate of 0.58×10^{-3} subs/site/year (95% CI: $0.51-0.65 \times 10^{-3}$), whereas that for the VOC stems was 2.45×10^{-3} subs/site/year (95% CI: $1.15-4.72 \times 10^{-3}$). The corresponding mean values in units of substitutions per month across the entire genome (subs/month) are 1.24 for the background and 6.11 for the foreground. As such, the VOC stems rate was around 4-fold higher than the background (mean 4.25, 95% CI: 2.61–8.19) (fig. 2).

Although the FLC stems model that assigned each VOC stem branch a different rate had very high uncertainty, it also suggested much higher rates for these branches. The mean background rate under this model was 0.55×10^{-3} subs/site/year (95% CI: $0.49-0.62 \times 10^{-3}$). The corresponding values for VOC were 8.47×10^{-3} subs/site/year (95% CI: $1.93-82.37 \times 10^{-3}$) for Alpha, 1.71×10^{-3} (95% CI: $0.34-33.20 \times 10^{-3}$) for Beta, 2.76×10^{-3} (95% CI: $1.21-13.23 \times 10^{-3}$) for Gamma, and 1.54×10^{-3} (95% CI: $0.62-7.35 \times 10^{-3}$) for Delta. Clearly, these estimates were several fold higher than that of the background branches, and in spite of their high uncertainty least 0.90 of the posterior density was higher than the mean background rate (fig. 2).

A key consideration is that the high uncertainty in the FLC stems model means that the actual values of rate estimates for VOC stem branches should be interpreted cautiously. The prior on all clock rates here is a continuous-time Markov chain (CTMC) reference prior, which consists of a Γ distribution with $\alpha = 0.5$ and $\beta = T$, where T is the tree length

(Ferreira and Suchard 2008; Wang and Yang 2014). Because the mean of a Γ distribution is α/β , under this prior the expectation is that the average substitution rate is $0.5/T$. Our estimate of T under this model had a mean of 85.6 (95% CI: 78.37–92.98), which results in a relatively wide distribution with an expected mean of around 5×10^{-3} subs/site/year. A comparison of this prior, the posterior for VOC stem branch rates, and the background rate illustrates that VOC branch rates deviate much less from the prior than the background rate does. Thus, VOC branch rate estimates under this model may be sensitive to the choice of prior (see supplementary figs. S2 and S3, Supplementary Material online). That is, the data may not be sufficiently informative to produce meaningful estimates of these parameters under this model.

The coefficient of rate variation for both relaxed clock models, UCG and UCLN, was indicative of departure from clocklike evolution in the data. To investigate whether VOC stem branch rates differed from the rest, we extracted individual branch rates and compared the VOC stem branch rates to the mean of all other branches. We found evidence that VOC stem branch rates were higher than the mean of other branches, with higher means values, but with very high uncertainty and 95% credible intervals that overlapped with the mean of other branches (fig. 3).

The mean substitution rate of branches other than the VOC stems was 0.65×10^{-3} subs/site/year (95% CI: $0.58-0.77 \times 10^{-3}$) in the UCLN and 0.69×10^{-3} subs/site/year (95% CI: $0.60-0.80 \times 10^{-3}$) for the UCG. In contrast, the VOC stem mean substitution rates for the UCLN were: 1.29×10^{-3} subs/site/year (95% credible interval, CI: $0.76-2.56 \times 10^{-3}$) for Alpha, 0.64×10^{-3} (95% CI: $0.32-1.57 \times 10^{-3}$) for Beta, 1.29×10^{-3} ($0.82-2.40 \times 10^{-3}$) for Gamma, and 1.06×10^{-3} (95% CI: $0.50-2.38 \times 10^{-3}$) for Delta, and with comparable values for the UCG. The quantile where VOC stems rates fell with respect to other branches also supported the finding that their rates were particularly high in most cases. In the UCLN, for Alpha 0.96 of posterior density had the stem rate in the top 75% of fastest evolving branches, with the corresponding numbers for the other VOCs being 0.25, 0.98, and 0.81 Beta, Gamma, and Delta, respectively, and with comparable values in the UCG (0.92, 0.45, 0.96, and 0.91; fig. 3).

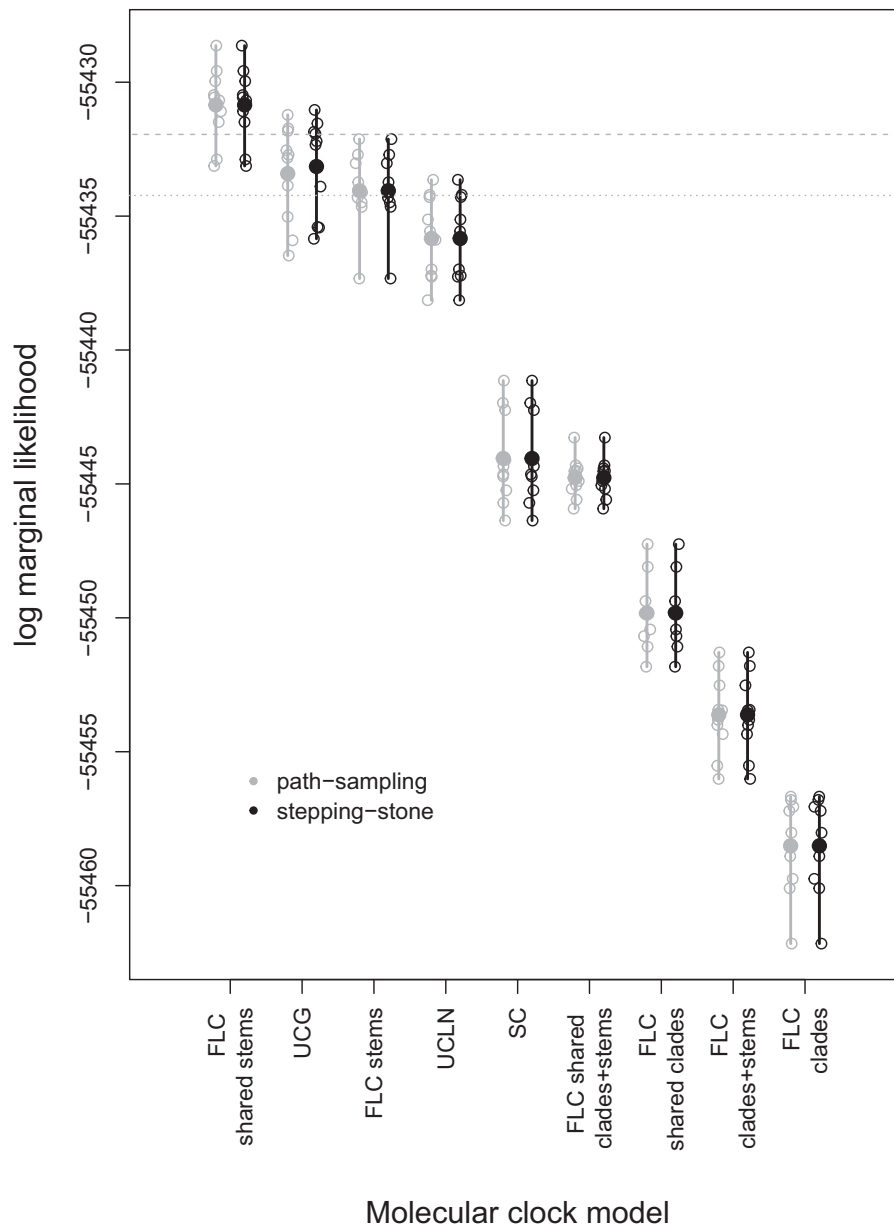


Fig. 1. Calculations of log marginal likelihoods for all molecular clock models using path sampling and stepping-stone. The hollow circles represent individual estimates, with ten replicates per model, and solid circles denote the mean value over replicates. The vertical lines represent the range of values in each case. The horizontal dashed line corresponds to a log BF of 1.1 (“substantial evidence”) relative to the mean log marginal likelihood of the best model (FLC shared stems), whereas the dotted line is the same value relative to the lowest log marginal likelihood of the best model.

The RLC model produced less clear results than the other molecular clock models. The maximum a posteriori number of rate changes was 4, with the 95% CI ranging between 2 and 5. However, the posterior probability of rate changes in VOC stem branches or clades was 0.0. Instead, rate changes were not consistently found on particular branches. It is conceivable that this model poses a heavy penalty on rate changes. In particular, there is a very large number of local clock configurations in these data, which may be impossible to visit under a standard Markov chain Monte Carlo analyses and may result in low statistical power to assess support for our hypotheses. This model had a substitution rate estimate that was

comparable with that of other models (mean 0.60×10^{-3} subs/site/year; 95% CI: $0.49\text{--}0.72 \times 10^{-3}$).

Emergence Time and Expected Genome Substitutions

We estimated the duration of time along VOC stem branches and the inferred total number of nucleotide substitutions along the complete genome. We focus on the best fitting model (FLC shared stems), with similar results for other models (supplementary fig. S4, Supplementary Material online). The duration of time along these branches represents the time required before VOCs started to diversify, but it is important to note that they are contingent on sampling bias,

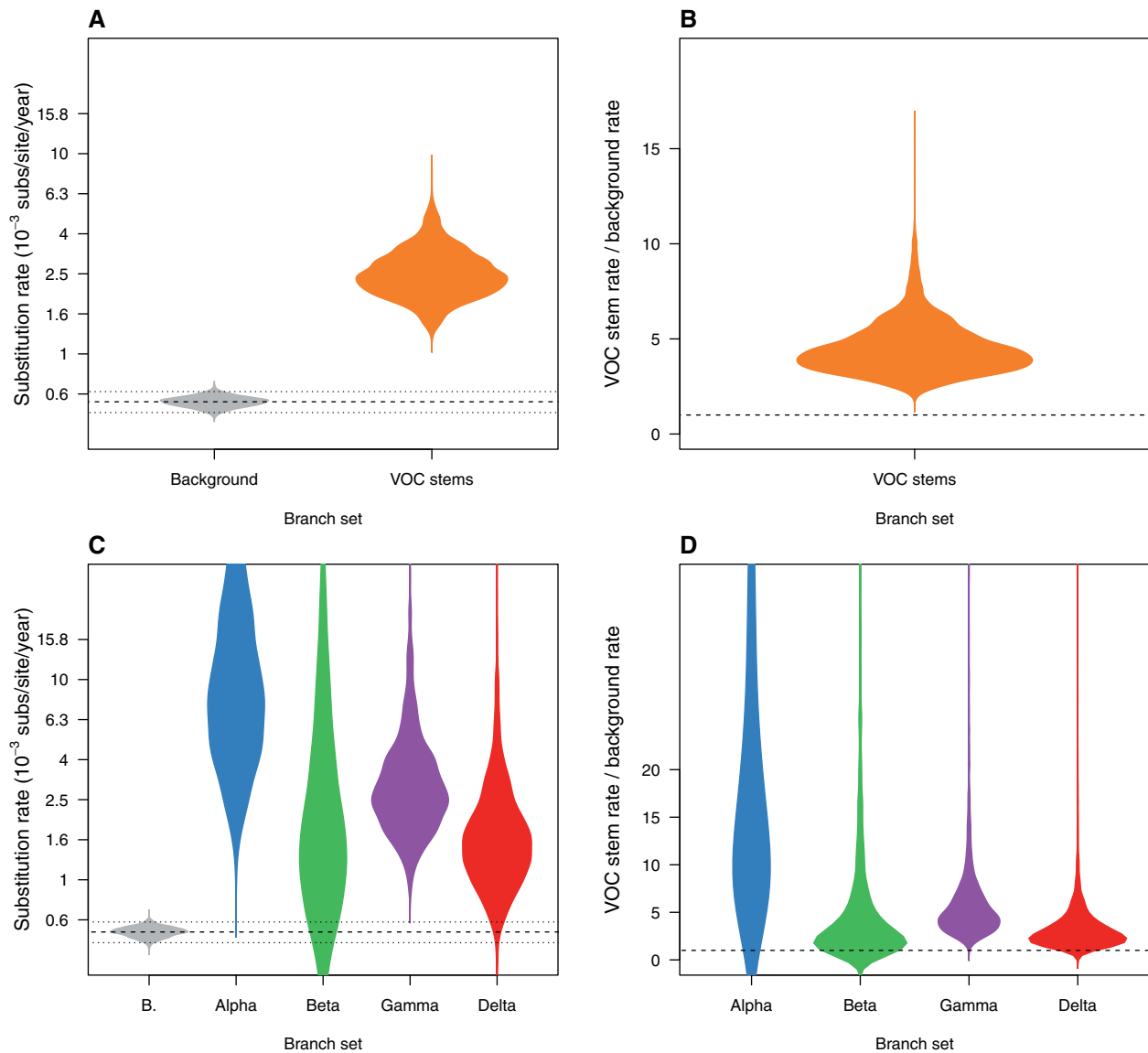


FIG. 2. Violin plots for posterior statistics of FLC. (A) is for a model where the stem branches of VOCs share a substitution rate that is different to that of the background (model “FLC shared stems” in [supplementary table S1](#) and [fig. S1, Supplementary Material online](#)). The substitution rate for VOCs stem branches is shown in orange and the background in gray. The dashed line represents the mean background rate and the dotted lines are the 95% credible interval. (B) is the ratio of the substitution rate for VOC stem branches and the background under the same model and the dashed line represents a value of 1.0 where the background and VOC stem rate would be the same. (C) and (D) show the corresponding statistics for the FLC stems model, where the stem branch of every VOC has a different rate. Abbreviation “B” stands for background.

and could therefore be shorter than estimated here. Under the FLC-shared stems model, the stem branch leading up to VOs were: 14 weeks (95% CI: 6–24) for Alpha, 4 (95% CI: 2–8) for Beta, 17 (95% CI: 8–28) for Gamma, and 6 (3–11) for Delta ([supplementary fig. S4, Supplementary Material online](#)).

The expected number of substitutions along the complete genome were: 21 (95% CI: 14–32) for Alpha, 6 (95% CI: 3–11) for Beta, 26 (95% CI: 18–35) for Gamma, and 9 (95% CI: 6–16) for Delta. Although, these numbers are loosely associated with the number of defining mutations, they are not directly comparable because they involve substitutions along the entire genome and they correspond to the inference from a standard phylogenetic substitution model (the GTR + Γ in this case).

Discussion

Our mean rate estimates over all lineages are somewhat lower than earlier estimates ([Duchene et al. 2020](#)), which is consistent with the notion that the virus has had time to evolve and to remove transient deleterious mutations since its emergence ([Ghafari et al. 2022](#)). Clearly, the molecular substitution rate of SARS-CoV-2 displays substantial variation among lineages, a pattern that has been apparent since early phylogenetic analyses of the virus ([Duchene et al. 2020](#)).

Substitution rate variation is sometimes stochastic in nature and pinpointing its causes is often difficult in empirical data. Our explicit hypothesis testing framework suggests that the emergence of VOCs explains much of the substitution

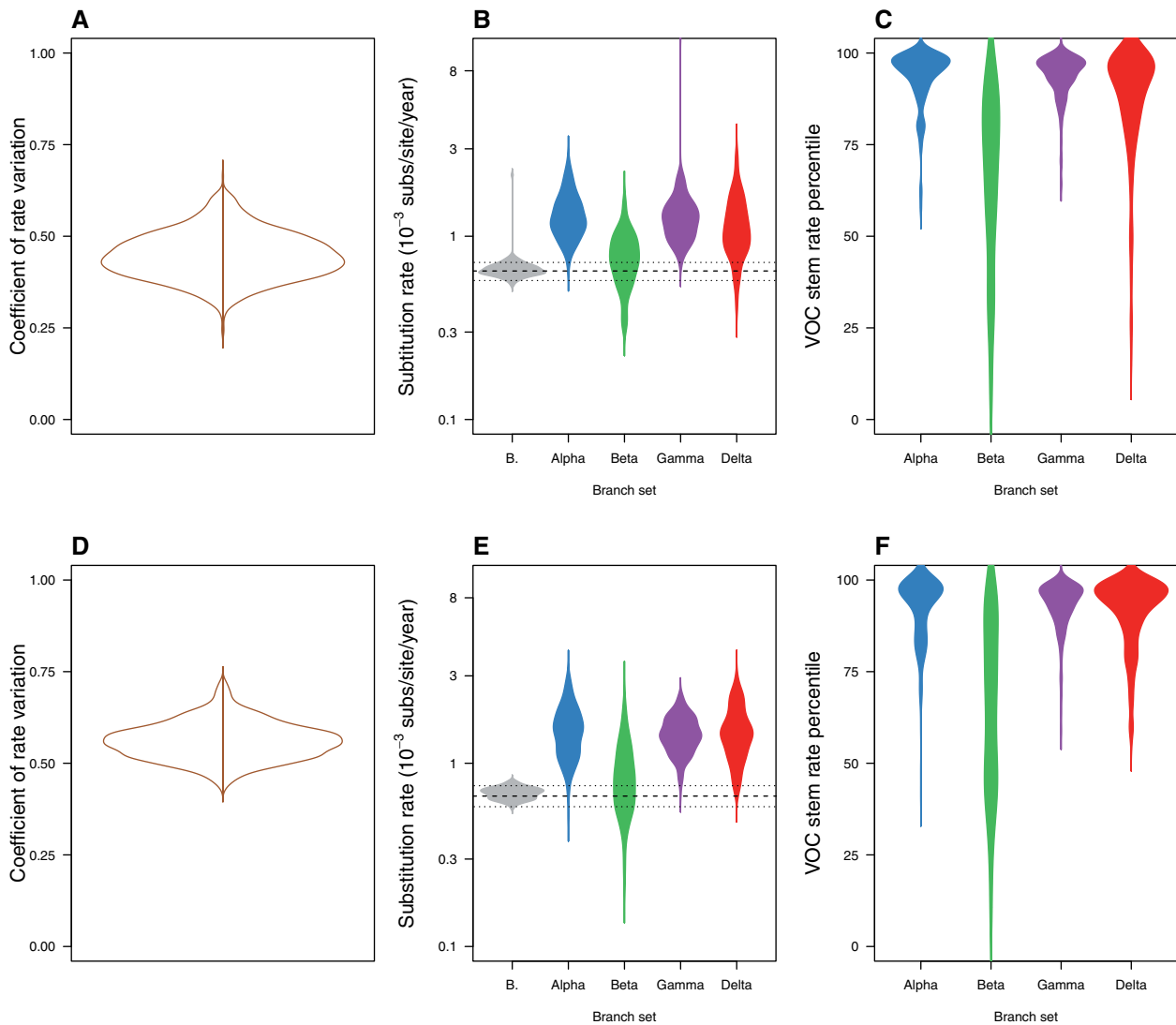


Fig. 3. Violin plots of posterior statistics for the uncorrelated relaxed clocks with lognormal (UCLN) and gamma (UCG) distributions (see [Supplementary Material online](#)). The top row, (A) through (C), is for the UCLN and the bottom row, (D) through (F), is for the UCG. (A) and (D) show the coefficient of rate variation, which is the standard deviation of branch rates divided by the mean rate, and indicates clock-like behavior when it is abutting zero ([Drummond et al. 2006](#); [Ho et al. 2015](#)). In (B) and (E), the substitution rate is shown for the stem branches of VOCs and for the mean of background branches (i.e., those that are not the stems of VOCs), abbreviated as “B.” The dashed line denotes the mean background rate, whereas the dotted lines represent the upper and lower 95% credible interval. (C) and (F) show the percentile in which stem branches for VOCs fall with respect to other branches. Note that the densities have been smoothed, but the maximum values are 100.

rate variation in the virus. This model testing framework has been previously used to understand viral evolution among host species in influenza ([Worobey et al. 2014](#)), and the host range SARS-CoV-2 and closely related viruses ([MacLean et al. 2021](#)). Here we used marginal likelihood estimators that have shown high accuracy ([Fourment et al. 2020](#)), but recent developments, including those based in sequential Monte Carlo ([Wang et al. 2020](#)), may improve statistical power for differentiating clock models. We suggest that model testing may be preferable to using highly parametric models, such as relaxed molecular clock models, for this purpose because they tend to have very high variance in substitution rates of particular branches. Recent advances in fitting relaxed and RLC models

may provide increased sensitivity and precision in branch specific rate estimates ([Douglas et al. 2021](#); [Fisher et al. 2021](#)).

We find compelling evidence that episodic, instead of long term, increases in the substitution rate underpin the emergence of VOCs, a process that is probably driven the action of natural selection. All models where VOC clades were assigned a different rate to the background had poor statistical fit, even when compared with the SC “null” model, providing further support for such rate increases to occur over a short period of time. The increase in substitution rate required to give rise to the four VOCs examined was estimated to be around 4-fold compared with the background, although such estimates may carry high uncertainty when estimated for individual

stem branches. Under these circumstances, the number of mutations required to give rise to a VOC, such as Alpha, would have accumulated in about 3 months, with some variants requiring a few weeks, such as Beta and Delta. These timescales appear plausible in chronic infections of SARS-CoV-2 (Harvey *et al.* 2021; Kemp *et al.* 2021), but other circumstances are also likely, for example, if transmission is infrequent and selection favors mutations that increase transmissibility between hosts.

Our genomic analyses demonstrate that signatures of increased substitution rates are detectable using phylogenetic methods and genome surveillance data. A recent study of reported increased evolutionary rates within sublineages of Gamma (Gräf *et al.* 2021), which prompts further investigation of within lineage evolution. However, the precise mechanism (ecological or intrahost) of how VOCs have emerged is still unclear. Elucidating these processes will require dense sampling between transmission chains, specifically in settings where transmission is unlikely and intra-host sequence data are available. Another important area that is currently under intense investigation is how natural selection shapes the emergence and persistence of VOCs (Martin *et al.* 2021; Tegally *et al.* 2021). Such studies may benefit from using explicit models where the substitution rate is treated as a function of environmental or ecological variables (Streicker *et al.* 2012). We recommend that further research focuses on early detection and understanding of the circumstances under which viral lineages with epidemiological impacts, such as VOCs, emerge.

Materials and Methods

Data Set Construction

We downloaded 100 randomly selected sequences in the global NextStrain SARS-CoV-2 build of August 2021 (Hadfield *et al.* 2018), from the GISAID database (Elbe and Buckland-Merrett 2017; Shu and McCauley 2017). This set of sequences did not include any of those belonging to the four VOCs (Alpha, Beta, Gamma, or Delta) and we also excluded samples drawn from nonhuman hosts. We then downloaded 20 randomly selected sequences from the four VOCs to generate a data set of 180 genomes, which we aligned using MAFFT (Katoh and Standley 2013). We ensured that the sequences consisted of complete genomes, with no stretches of more than 10 Ns and excluding those with low coverage (see [supplementary material, Supplementary Material online](#)). To verify that samples classified as VOCs were correctly assigned as such, we estimated a phylogenetic tree using maximum likelihood as implemented in IQ-TREE2 (Minh *et al.* 2020), using the GTR + Γ substitution model and with approximate Bayes branch support (Anisimova *et al.* 2011). We ensured that all VOCs were monophyletic with an approximate Bayes support of at least <0.95 .

Bayesian Phylogenetic Analyses

Our Bayesian analyses require specifying a substitution model, a tree prior and priors for all parameters in BEAST 1.10 (Suchard *et al.* 2018). We chose the GTR + Γ_4 substitution

model and a coalescent exponential tree prior. Although the tree prior is not necessarily realistic here, it is expected to have little impact in molecular clock estimates (Ritchie *et al.* 2017). Moreover, it can accommodate changes in population size via the exponential growth function and it is fully parametric, meaning that setting proper priors for all parameters is possible. To calibrate the molecular clock, we specified the sequence sampling times. The FLC models require constraining monophyly of VOCs, which we also did for other clock models to ensure that the prior on tree topology was the same.

We used the default priors for the substitution model. The coalescent exponential tree prior has two parameters, the scaled population size, Φ , and the growth rate r . The scaled population size is proportional to the number of infected individuals at present divided by twice the coalescent rate, λ (i.e., $\Phi = \frac{l(0)}{2\lambda}$), and the growth rate is inversely proportional to the doubling time by a factor of $\log(2)$ (doubling time = $\frac{\log(2)}{r}$) (Volz *et al.* 2009; Boskova *et al.* 2014). We used priors with relatively low information content for these two parameters. For Φ , we used an exponential distribution with mean 10^5 , whereas for r , we used a Laplace distribution with location 0 and scale 100. For all molecular clock rates, we used a CTMC reference prior (Ferreira and Suchard 2008; Wang and Yang 2014). The UCLN and UCG models have an additional parameter; the standard deviation of the lognormal distribution, and the shape of the Γ distribution. For these parameters, we specified an exponential prior with mean 0.33. We ran our analyses for using a Markov chain Monte Carlo of length 5×10^7 , sampling every 5×10^3 and discarding 10% of the chain as burn-in. We repeated the analyses once to verify convergence of independent chains and we ensured that the effective sample size of all parameters was at least 200.

Marginal Likelihood Estimation

We used two techniques to infer the log marginal likelihood: path sampling and stepping-stone (Gelman and Meng 1998; Lartillot and Philippe 2006; Xie *et al.* 2011), which have been found to have high performance in differentiating models in phylogenetics (Baele *et al.* 2012, 2013; Fourment *et al.* 2020), reviewed by Baele and Lemey (2014) and Oaks *et al.* (2019). We chose these estimators over the more recently developed and highly accurate generalized stepping-stone because the latter requires a working genealogical distribution (Baele *et al.* 2016), which is not trivial here due to the monophyletic constraints in our models. Our estimation setup had 200 path steps distributed according to quantiles from a β distribution with parameter $\alpha = 0.3$, with each of the resulting 201 power posterior inferences running for 10^6 iterations. We repeated these analyses ten times to assess variation in these calculations and used the log BF of the mean values. Our model testing approach considered the UCLN, SC, and all FLC models in [table 1](#) and [supplementary material, Supplementary Material online](#). We did not calculate log marginal likelihoods for the RLC because this is a model averaging method, where the number of parameters is less tractable than in other models and thus it is difficult to conceive proper

priors for all parameters, a fundamental aspect of Bayesian model selection.

Supplementary Material

Supplementary data are available at *Molecular Biology and Evolution* online.

Acknowledgments

This work was supported by the Australian Research Council (DE190100805) and the Australian Medical Research Future Fund (MRF9200006). This research was undertaken using the LIEF HPC GPGPU facility hosted at the University of Melbourne. This Facility was established with the assistance of LIEF Grant LE170100200. We acknowledge efforts by originating and submitting laboratories for the sequence data in GISAID EpiCoV on which our analyses are based. We are grateful to Prof. Edward Holmes for useful suggestions and comments on ideas developed in this study. We also thank two anonymous reviewers for useful suggestion and comments of earlier versions of this manuscript.

Data Availability

The data underlying this article are available in GISAID at gisaid.org, and all accession numbers are provided in [Supplementary Material online](#).

References

Abdool Karim SS, de Oliveira T. 2021. New SARS-CoV-2 variants—clinical, public health, and vaccine implications. *N Engl J Med*. 384(19):1866–1868.

Anisimova M, Gil M, Dufayard J-F, Dessimoz C, Gascuel O. 2011. Survey of branch support methods demonstrates accuracy, power, and robustness of fast likelihood-based approximation schemes. *Syst Biol*. 60(5):685–699.

Baele G, Lemey P. 2014. Bayesian model selection in phylogenetics and genealogy-based population genetics. In: Chen M, Kuo L, and Lewis P, editors. *Bayesian phylogenetics, methods, algorithms, and applications*. Chapter 4. Boca Raton (FL): CRC Press. p. 59–93.

Baele G, Lemey P, Bedford T, Rambaut A, Suchard MA, Alekseyenko AV. 2012. Improving the accuracy of demographic and molecular clock model comparison while accommodating phylogenetic uncertainty. *Mol Biol Evol*. 29(9):2157–2167.

Baele G, Lemey P, Suchard MA. 2016. Genealogical working distributions for Bayesian model testing with phylogenetic uncertainty. *Syst Biol*. 65(2):250–264.

Baele G, Lemey P, Vansteelandt S. 2013. Make the most of your samples: Bayes factor estimators for high-dimensional models of sequence evolution. *BMC Bioinformatics* 14(1):85.

Boskova V, Bonhoeffer S, Stadler T. 2014. Inference of epidemiological dynamics based on simulated phylogenies using birth-death and coalescent models. *PLoS Comput Biol*. 10(11):e1003913.

Bromham L, Duchêne S, Hua X, Ritchie AM, Duchêne DA, Ho SY. 2018. Bayesian molecular dating: opening up the black box. *Biol Rev Camb Philos Soc*. 93(2):1165–1191.

CDC. 2021. COVID-19: SARS-CoV-2 variant classifications and definitions. Atlanta (GA): US Department of Health and Human Services, CDC. Available from: <https://www.cdc.gov/coronavirus/2019-ncov/cases-updates/variant-surveillance/variant-info.html>.

Dearlove B, Lewitus E, Bai H, Li Y, Reeves DB, Joyce MG, Scott PT, Amare MF, Vasan S, Michael NL, et al. 2020. A SARS-CoV-2 vaccine candidate would likely match all currently circulating variants. *Proc Natl Acad Sci U S A*. 117(38):23652–23662.

Dellicour S, Durkin K, Hong SL, Vanmechelen B, Martí-Carreras J, Gill MS, Meex C, Bontems S, André E, Gilbert M, et al. 2021. A phylogenetic workflow to rapidly gain insights into the dispersal history and dynamics of SARS-CoV-2 lineages. *Mol Biol Evol*. 38(4):1608–1613.

Douglas J, Zhang R, Bouckaert R. 2021. Adaptive dating and fast proposals: revisiting the phylogenetic relaxed clock model. *PLoS Comput Biol*. 17(2):e1008322.

Drummond AJ, Ho SYW, Phillips MJ, Rambaut A. 2006. Relaxed phylogenetics and dating with confidence. *PLoS Biol*. 4(5):e88.

Drummond AJ, Suchard MA. 2010. Bayesian random local clocks, or one rate to rule them all. *BMC Biol*. 8(1):114.

Duchene S, Featherstone L, Haritopoulou-Sinanidou M, Rambaut A, Lemey P, Baele G. 2020. Temporal signal and the phylogenetic threshold of SARS-CoV-2. *Virus Evol*. 6(2):veaa061.

Elbe S, Buckland-Merrett G. 2017. Data, disease and diplomacy: GISAID's innovative contribution to global health. *Glob Chall*. 1(1):33–46.

Eurosurveillance Editorial Team. 2021. Updated rapid risk assessment from ECDC on the risk related to the spread of new SARS-CoV-2 variants of concern in the EU/EEA—first update. *Eurosurveillance*. 26(3):2101211.

Faria NR, Mellan TA, Whittaker C, Claro IM, Candido D, D S, Mishra S, Crispim MA, Sales FC, Hawryluk I, McCrone JT, et al. 2021. Genomics and epidemiology of the p. 1 SARS-CoV-2 lineage in Manaus, Brazil. *Science* 372(6544):815–821.

Ferreira MA, Suchard MA. 2008. Bayesian analysis of elapsed times in continuous-time Markov chains. *Can J Stat*. 36(3):355–368.

Fisher AA, Ji X, Nishimura A, Lemey P, Suchard MA. 2021. Shrinkage-based random local clocks with scalable inference. arXiv preprint arXiv:2105.07119.

Fourment M, Darling AE. 2018. Local and relaxed clocks: the best of both worlds. *PeerJ*. 6:e5140.

Fourment M, Magee AF, Whidden C, Bilge A, Matsen FA IV, Minin VN. 2020. 19 dubious ways to compute the marginal likelihood of a phylogenetic tree topology. *Syst Biol*. 69(2):209–220.

Gelman A, Meng X-L. 1998. Simulating normalizing constants: from importance sampling to bridge sampling to path sampling. *Stat Sci*. 13:163–185.

Ghafari M, du Plessis L, Raghwanji J, Bhatt S, Xu B, Pybus O, Katzourakis A. 2022. Purifying selection determines the short-term time dependency of evolutionary rates in SARS-CoV-2 and pH1N1 influenza. *Mol Biol Evol*. Advance Access published January 17, 2022, doi: 10.1093/molbev/msac009.

Gräf T, Bello G, Venas TMM, Pereira EC, Paixão ACD, Appolinario LR, Lopes RS, Mendonça A. C D F, da Rocha ASB, Motta FC, et al. 2021. Identification of a novel SARS-CoV-2 p. 1 sub-lineage in Brazil provides new insights about the mechanisms of emergence of variants of concern. *Virus Evol*. 7(2):veab091.

Hadfield J, Megill C, Bell SM, Huddleston J, Potter B, Callender C, Sagulenko P, Bedford T, Neher RA. 2018. Nextstrain: real-time tracking of pathogen evolution. *Bioinformatics* 34(23):4121–4123.

Harvey WT, Carabelli AM, Jackson B, Gupta RK, Thomson EC, Harrison EM, Ludden C, Reeve R, Rambaut A, Peacock SJ, et al. 2021. SARS-CoV-2 variants, spike mutations and immune escape. *Nat Rev Microbiol*. 19(7):409–424.

Ho SY, Duchêne S. 2014. Molecular-clock methods for estimating evolutionary rates and timescales. *Mol Ecol*. 23(24):5947–5965.

Ho SY, Duchêne S, Duchêne D. 2015. Simulating and detecting autocorrelation of molecular evolutionary rates among lineages. *Mol Ecol Resour*. 15(4):688–696.

Ho SY, Lanfear R, Bromham L, Phillips MJ, Soubrier J, Rodrigo AG, Cooper A. 2011. Time-dependent rates of molecular evolution. *Mol Ecol*. 20(15):3087–3101.

Kass RE, Raftery AE. 1995. Bayes factors. *J Am Statist Assoc*. 90(430):773–795.

Katoh K, Standley DM. 2013. MAFFT multiple sequence alignment software version 7: improvements in performance and usability. *Mol Biol Evol*. 30(4):772–780.

Kemp SA, Collier DA, Datir RP, Ferreira IA, Gayed S, Jahun A, Hosmillo M, Rees-Spear C, Mlcochova P, Lumb IU, et al. 2021. SARS-CoV-2

- evolution during treatment of chronic infection. *Nature* 592(7853):277–282.
- Konings F, Perkins MD, Kuhn JH, Pallen MJ, Alm EJ, Archer BN, Barakat A, Bedford T, Bhiman JN, Caly L, et al. 2021. SARS-CoV-2 variants of interest and concern naming scheme conducive for global discourse. *Nat Microbiol.* 6:821–823.
- Kraemer MU, Hill V, Ruis C, Dellicour S, Bajaj S, McCrone JT, Baele G, Parag KV, Battle AL, Gutierrez B, et al. 2021. Spatiotemporal invasion dynamics of SARS-CoV-2 lineage b. 1.1. 7 emergence. *Science* 373(6557):889–895.
- Lartillot N, Philippe H. 2006. Computing Bayes factors using thermodynamic integration. *Syst Biol.* 55(2):195–207.
- MacLean OA, Lytras S, Weaver S, Singer JB, Boni MF, Lemey P, Kosakovsky Pond SL, Robertson DL. 2021. Natural selection in the evolution of SARS-CoV-2 in bats created a generalist virus and highly capable human pathogen. *PLoS Biol.* 19(3):e3001115.
- Martin DP, Weaver S, Tegally H, San JE, Shank SD, Wilkinson E, Lucaci AG, Giandhari J, Naidoo S, Pillay Y, et al. 2021. The emergence and ongoing convergent evolution of the SARS-CoV-2 n501y lineages. *Cell* 184(20):5189–5200.
- Mascola JR, Graham BS, Fauci AS. 2021. SARS-CoV-2 viral variants—tackling a moving target. *JAMA* 325(13):1261–1262.
- Minh BQ, Schmidt HA, Chernomor O, Schrempf D, Woodhams MD, Von Haeseler A, Lanfear R. 2020. Iq-tree 2: new models and efficient methods for phylogenetic inference in the genomic era. *Mol Biol Evol.* 37(5):1530–1534.
- Nelson G, Buzko O, Spilman PR, Niazi K, Rabizadeh S, Soon-Shiong PR. 2021. Molecular dynamic simulation reveals E484K mutation enhances spike RBD-ACE2 affinity and the combination of E484K, K417N and N501Y mutations (501Y. v2 variant) induces conformational change greater than N501Y mutant alone, potentially resulting in an escape mutant. *BioRxiv*.
- Oaks J, Cobb KF, Minin VN, Leaché AD. 2019. Marginal likelihoods in phylogenetics: a review of methods and applications. *Syst Biol.* 68(5):681–697.
- Pekar J, Worobey M, Moshiri N, Scheffler K, Wertheim JO. 2021. Timing the SARS-CoV-2 index case in Hubei province. *Science* 372(6540):412–417.
- Plante JA, Liu Y, Liu J, Xia H, Johnson BA, Lokugamage KG, Zhang X, Muruato AE, Zou J, Fontes-Garfias CR, et al. 2021. Spike mutation d614g alters SARS-CoV-2 fitness. *Nature* 592(7852):116–121.
- Rambaut A, Holmes EC, O’Toole Á, Hill V, McCrone JT, Ruis C, du Plessis L, Pybus OG. 2020. A dynamic nomenclature proposal for SARS-CoV-2 lineages to assist genomic epidemiology. *Nat Microbiol.* 5(11):1403–1407.
- Ritchie AM, Lo N, Ho SY. 2017. The impact of the tree prior on molecular dating of data sets containing a mixture of inter- and intraspecies sampling. *Syst Biol.* 66(3):413–425.
- Shu Y, McCauley J. 2017. GISAID: global initiative on sharing all influenza data—from vision to reality. *Eurosurveillance* 22(13):30494.
- Sinsheimer JS, Lake JA, Little RJ. 1996. Bayesian hypothesis testing of four-taxon topologies using molecular sequence data. *Biometrics* 52(1):193–210.
- Streicker DG, Lemey P, Velasco-Villa A, Rupprecht CE. 2012. Rates of viral evolution are linked to host geography in bat rabies. *PLoS Pathog.* 8(5):e1002720.
- Suchard MA, Lemey P, Baele G, Ayres DL, Drummond AJ, Rambaut A. 2018. Bayesian phylogenetic and phylodynamic data integration using beast 1.10. *Virus Evol.* 4(1):vey016.
- Tegally H, Wilkinson E, Giovanetti M, Iranzadeh A, Fonseca V, Giandhari J, Doolabh D, Pillay S, San EJ, Msomi N, et al. 2021. Detection of a SARS-CoV-2 variant of concern in South Africa. *Nature* 592(7854):438–443.
- Viana R, Moyo S, Amoako DG, Tegally H, Scheepers C, Lessells RJ, Giandhari J, Wolter N, Everatt J, Rambaut A, et al. 2022. Rapid epidemic expansion of the SARS-CoV-2 Omicron variant in southern Africa. *Nature*. Advance Access published January 20, 2022, doi: 10.1038/s41586-022-04411-y.
- Volz E, Hill V, McCrone JT, Price A, Jorgensen D, O’Toole Á, Southgate J, Johnson R, Jackson B, Nascimento FF, et al. 2021. Evaluating the effects of SARS-CoV-2 spike mutation d614g on transmissibility and pathogenicity. *Cell* 184(1):64–75.
- Volz EM, Kosakovsky Pond SL, Ward MJ, Leigh Brown AJ, Frost SD. 2009. Phylodynamics of infectious disease epidemics. *Genetics* 183(4):1421–1430.
- Wang L, Wang S, Bouchard-Côté A. 2020. An annealed sequential Monte Carlo method for Bayesian phylogenetics. *Syst Biol.* 69(1):155–183.
- Wang Y, Yang Z, Chen M-H, Kuo L, Lewis PO. 2014. Priors in Bayesian phylogenetics, Bayesian phylogenetics: methods, algorithms, and applications. Boca Raton: Chapman and Hall/CRC. p. 5–23.
- Worobey M, Han G-Z, Rambaut A. 2014. A synchronized global sweep of the internal genes of modern avian influenza virus. *Nature* 508(7495):254–257.
- Xie W, Lewis PO, Fan Y, Kuo L, Chen M-H. 2011. Improving marginal likelihood estimation for Bayesian phylogenetic model selection. *Syst Biol.* 60(2):150–160.
- Yoder AD, Yang Z. 2000. Estimation of primate speciation dates using local molecular clocks. *Mol Biol Evol.* 17(7):1081–1090.
- Zuckerandl E, Pauling L. 1962. Molecular disease, evolution and genic heterogeneity. In: Kasha M, Pullman B, editors. *Horizons in biochemistry*. New York: Academic Press. p. 189–225.
- Zuckerandl E, Pauling L. 1965. Evolutionary divergence and convergence in proteins. In: Bryson V, Vogel HJ, editors. *Evolving genes and proteins*. New York: Academic Press. p. 97–166.